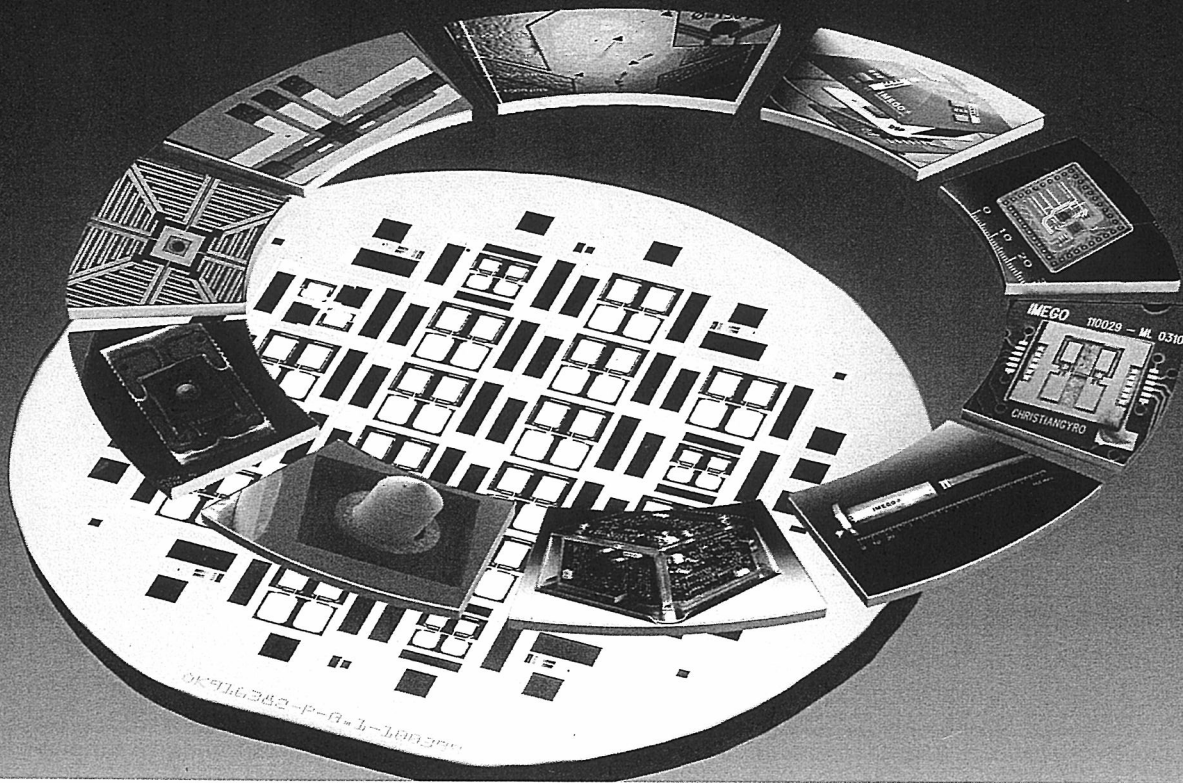




16th MME

MicroMechanics Europe Workshop

4-6 September 2005, Göteborg, Sweden



CHALMERS

MC2
Microtechnology and Nanoscience

IMEGO 
Applied Micro Sensor Systems

Knowledge Foundation



Vetenskapsrådet



City of
Göteborg



**EXPERIMENTAL INVESTIGATION OF FRICTION FACTORS
FOR GAS FLOW ACROSS DENSE PILLAR MATRICES IN MICROCHANNELS**

**S. Vanapalli¹, J.F. Burger², T.T Veenstra², H.J. Holland², G.C.F. Venhorst², H.V. Jansen¹,
H.J.M ter Brake², M. Elwenspoek¹**

¹Transducers Science and Technology Group, ²Low Temperature Group,
MESA+ Research Institute, University of Twente, Enschede, The Netherlands

s.vanapalli@ewi.utwente.nl

Abstract — *An experimental study of low Reynolds number gas flow across pillars in a microchannel is presented. Various geometries of pillars are considered for systematic comparison. This is for the first time such an investigation is done. The pillars 25 μm in diameter and height of 230 μm are dry etched in silicon. A 4-point pressure drop measurement setup is used to avoid measuring losses in fittings. Among various geometries considered, shifted sine pattern and rhombus shaped structures with an aspect ratio of 1/3 have the lowest friction factor and circle staggered arrangement has the highest friction factor.*

Key Words: *Friction factor, Micro-gas flow, regenerator, microcooler, MEMS*

I INTRODUCTION

Miniaturization of refrigerators has been a study of interest for several years. One of the first successful realizations of cold stage was reported by W. A. Little [1] and J.F. Burger [2] employing a recuperative refrigeration cycle. Regenerative cycles are of special interest owing to their higher theoretical efficiencies and possibility of miniaturizing the complete system including the compressor. Preliminary study on miniaturization and realization are reported [2-5]. Applications of these coolers include but are not limited to cooling of vibration-sensitive detectors in space missions, cooling of low-noise amplifiers, microelectronic components, miniature sensors, and microsystems. One of the core components of the regenerative coolers is the regenerator. A regenerator is a kind of heat exchanger where heat is transferred between the gas and solid in one part of a cycle and backwards in another part while maintaining a temperature gradient across the cooler [6]. One of the primary design goals for a regenerator is to identify a matrix structure in the regenerator with good heat transfer and low-pressure drop.

In the design of heat exchangers with cooling liquids, accurate knowledge of the friction characteristics of the heat transfer surface is

relatively unimportant because of the low power requirement for pumping high-density fluids. For gases, however, because of low density, the friction power per unit mass flow rate is greatly multiplied. Thus the friction characteristic of the surface assumes an importance equal to that of the heat transfer characteristic. The friction characteristic needed is the friction factor, which is a function of the flow geometry and the Reynolds number. One of the first investigations for friction characteristics in micro channels is reported by Pffaler et. al [7]. Computational fluid dynamic simulations of matrix elements are reported by I. Rulich et al [8].

Friction factors for rectangular channels can be analytically determined. No analytical solution exists for channels with pillars. In this paper we report an experimental approach to determine friction factor. The definitions, fabrication and results from experiments for pillars in microchannels are reported.

II DEFINITIONS

Some definitions are introduced for a common treatment of flow-friction data for all geometric shapes considered. This is to avoid the confusion often encountered with a large number of arbitrarily defined parameters. Consider a rectangular volume V , with height H , width W and length L filled with matrix elements occupying volume V_{matrix} and has a total surface area A_s . The cross-sectional area is $A=W.H$

The porosity is defined as,

$$\varepsilon = 1 - V_{\text{matrix}}/V \quad (1)$$

Hydraulic Diameter,

$$D_h = 4 \varepsilon V / A_s \quad (2)$$

Free flow velocity,

$$U = \dot{m} / \rho A \quad (3)$$

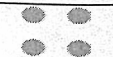







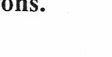
Pattern	Code	Porosity	D_h	L	a	b	c	d	
Circle Aligned	CA	0.82	109	9900	25	25	50	50	
Circle Staggered	CS	0.82	109	9900	25	25	100	50	
Square Staggered	SS	0.82	107	9900	25	25	112	56	
Ellipse 1/3 Staggered	ES1	0.62	56	9900	75	25	92	80	
Ellipse 1/4 Staggered	ES2	0.66	51	9900	80	20	90	75	
Shifted Sine Staggered	SSS	0.53	51	10048	75	25	75	50	
Rhombus Staggered	RSC	0.66	48	9975	75	25	82	76	
Eye Staggered	ES	0.83	102	13800	68	24	82	128	
Rhombus Staggered	RS	0.66	48	9900	75	25	82	76	

Table 1. The information of geometric and hydraulic parameters. All dimensions are in microns.

Mean flow area,

$$A_m = \varepsilon A \quad (4)$$

Mean velocity,

$$U_m = U / \varepsilon \quad (5)$$

Reynolds number

$$Re = \rho U_m D_h / \mu \quad (6)$$

Pressure drop,

$$\Delta P = f \cdot \frac{L}{D_h} \cdot \frac{1}{2} \rho U_m^2 \quad (7)$$

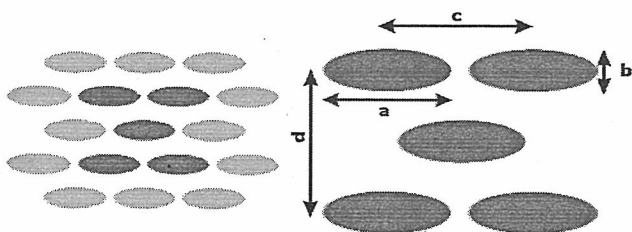


Figure 1. Description of a generic unit cell

Several geometries namely circular, square, elliptical, eye, shifted sine, rhombus shaped are considered. Fig.1 is the description of a unit cell of a generic shaped element. The porosity, hydraulic diameter and dimensions for all the geometries are summarized in Tab.1.

III FABRICATION

The schematic of the device is shown in Fig.2. It consists of two wafers bonded together to confine a channel with matrix structures. The bottom wafer is the standard silicon wafer with pillars etched with DRIE Bosch process [9]. The etch parameters of the Bosch process are optimiz

ed to obtain an almost vertical sidewalls. SEM picture of the matrix and cross-section of the walls is shown in Fig.3. The top wafer is a 1.1 mm thick borofloat glass wafer. Interconnection channels are powder blasted [10] to a depth of $\sim 750 \mu\text{m}$. The top and bottom wafers are anodic bonded and diced to realize individual samples. Glass capillaries with an inner diameter of $530 \mu\text{m}$ and an outer diameter of $680 \mu\text{m}$ are glued with Torr Seal [11] into the interconnection channels blasted previously in the glass wafer. Fig. 4 shows the mounted sample.

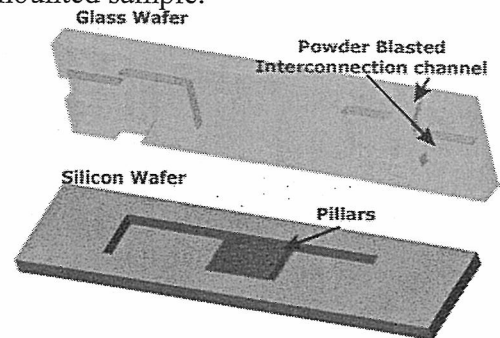


Figure 2. Schematic of the device

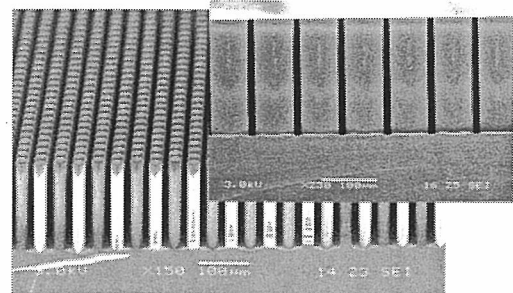


Figure 3. SEM pictures of etched samples. The top picture is the cross-section of the pillars.

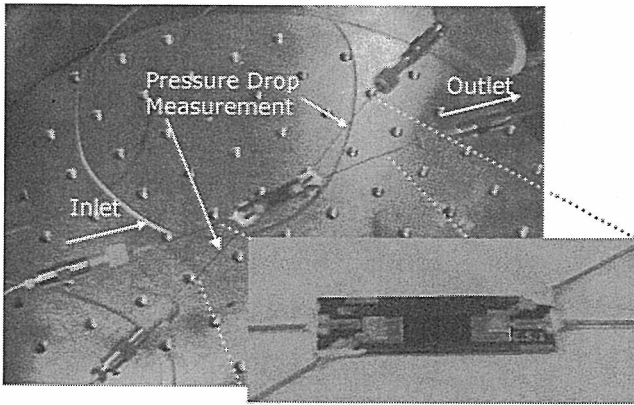


Figure 4. Mounted and a closed view of the sample

IV EXPERIMENTS

IV.1 EXPERIMENTAL SETUP

The experimental apparatus is depicted schematically in Fig. 5. Experimental apparatus consists of a test sample, regulated pressurized bottle, absolute pressure sensor, differential pressure sensor and a mass flow controller. With this configuration the absolute pressure could be adjusted with the pressure regulator and at the same time the mass flow through the valve could be adjusted with the flow controller.

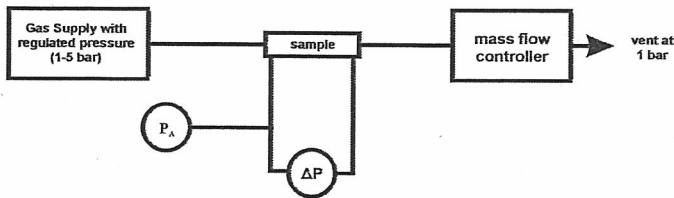


Figure 5. Schematic of experimental setup

The resulting pressure drop over the sample was measured with a differential pressure sensor with a range of 1 psi (1bar =14.5 psi) fabricated by Honeywell [12]. To avoid measuring pressure drop due to fittings we adapted to a 4-point set-up. In the experiments reported here we used nitrogen gas. The experimental procedure consist of setting the mass flow to a certain value and then vary the inlet pressure by regulating the valve of the gas bottle; once the flow has stabilized the pressure drop values are recorded. This procedure is repeated for different values of mass flow and absolute pressure.

IV.2 RESULTS

One of the first steps is to investigate the pressure losses due to entrance effects. From Eqn. 7, the pressure drop over the sample scales

with length, L . So we designed samples with two different lengths, $L1$ and $L2$ ($L2=2 \times L1$). Experiments were carried out to measure pressure drop and mass flow for the above samples. Fig. 6 is the graph of pressure drop as a function of mass flow rate for the two samples. The pressure drop measured with the twice-long sample is twice as much. The offset in Fig. 6 is due to the offset in the pressure transducer.

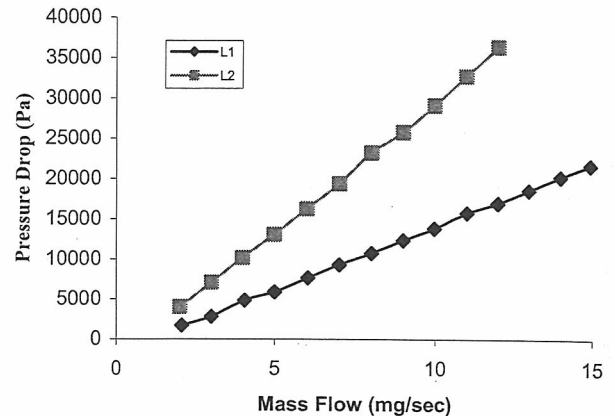


Figure 6. Pressure drop versus mass flow for two different regenerator length showing negligible entrance effects.

The next parameter to investigate is the effect of pillar arrangement on the pressure drop. Circular aligned and staggered patterns with identical porosity and dimensions are tested. Fig. 7 is the plot of pressure drop vs mass flow for circular aligned and staggered arrangements. The staggered arrangement has a higher pressure drop compared to aligned patterns.

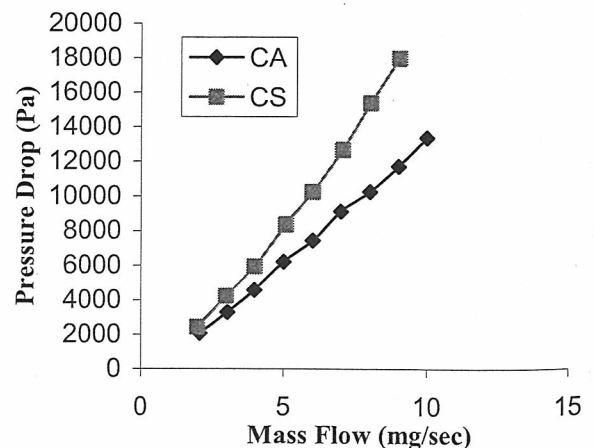


Figure 7. A comparison between the aligned and staggered arrangements for pressure drop.

To compare various matrices it is convenient to use non-dimensional parameters (friction factor, f and Reynolds Number, Re). From experiments we measured pressure drop and mass flow. Eqn. 1-7 are used to compute friction factor and Reynolds number. Fig. 8 shows the friction factors vs Reynolds number for all the shapes, which are plotted on a logarithmic scale.

Circular, Square, Eye staggered arrangements have the highest friction factors, followed by elliptical shaped, shifted sine and rhombus connected, the least is rhombus disconnected.

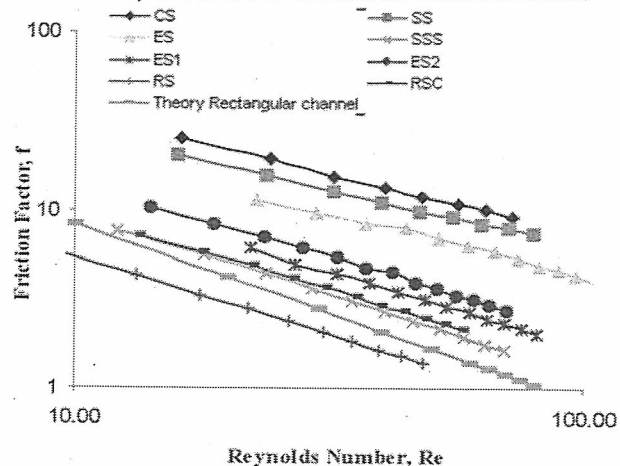


Figure 8. Calculated friction factors for all the configurations

The friction factor for rectangular channel can be theoretically calculated. The friction coefficient, $C = f \cdot Re$ is 84 for a rectangular channel with an aspect ratio of 9 [13]. In Fig 8. we included the plot of friction factor for a rectangular channel. It can be seen that the shifted sine, rhombus patterns have friction factors very close to that of the rectangular channel. A slightly higher friction factor is due to a larger length, which is due to the serpentine nature of these channels. Hence, one of the most influential parameter is the variation of cross-sectional area in the longitudinal direction. Shifted Sine and Rhombus pattern have a constant cross-sectional area and hence low friction factors. The low friction factor exhibited by rhombus-disconnected pattern could be attributed to a lower viscous force because of the absence of a mechanical boundary connecting the two pillars. Shifted sine connected has a lower friction factor compared to shifted rhombus pattern because of absence of sharp edges. When the mechanical

boundary connecting the shifted sine pattern is removed, it might have the lowest friction factor.

V CONCLUSION

Flow resistance of gas across a number of geometric shapes has been studied. A series of various shaped pillars has been fabricated and characterized. Four point pressure drop measurement provided a good method to measure pressure drop contribution only due to pillars. Three influential parameters for the hydraulic resistance are hydraulic diameter, matrix arrangement and shape of pillars. Among aligned and staggered patterns it is found that staggered arrangement has higher pressure drop. The shifted sine and rhombus pattern is found to have the lowest friction factor, which is closer to the theoretical values of friction factor for rectangular channels. It turns out that velocity changes attributed to changes in cross sectional area are very influential on the pressure drop.

REFERENCES

- [1] W.A. Little, "Microminiature Refrigeration", Rev. Sci. Instrum., vol. 55, no. 5, 1984.
- [2] J.F. Burger, 'Cryogenic Microcooling', Phd thesis, University of Twente, The Netherlands.
- [3] Matthew E. Maron, "Micro-Scale Regenerative Heat Exchanger", Conference on Micro-Nano-Technologies for Aerospace Applications, 2004, AIAA-2004-6730.
- [4] Philippe Nika et al, "An integrated pulse tube refrigerator device with micro exchangers: design and experiments", Int. Journal of Thermal Sciences, 42, pp 1029-1045, 2003.
- [5] N. Nakajima et al. "Study on Micro Engines-Miniaturizing Stirling Engines for Actuators and Heatpumps", proceedings IEEE MEMS, pp. 145-148, 1989.
- [6] G. Walker, 'Cryocooler', Plenum Press, New York, 1983
- [7] J. Pfahler, H.Lau, and J. Zemel, "Liquid and Gas Transport in Small Channels", Sensors and Actuators, Vol 19, pp. 149-157, November 1990.
- [8] I. Ruelich et al., Investigations on Regenerative Heat Exchangers, International Cryocooler Conference 10.
- [9] F.Laermer, D.Schilp, Method of anisotropically etching silicon, Licensed from Robert Bosch GmbH: Patent US5501893
- [10] H. Wensink et al, "High resolution powder blast micromachining", Proc. IEEE Workshop on MEMS, Japan, 2000.
- [11] Torr Seal, Varian Vacuum Technologies, 121 Hartwell Avenue, Lexington, MA 02421, USA.,
- [12] Product code, 26PCCFA6D, www.honeywell.com
- [13] W. M. Kays and A. L. London, 'Compact Heat Exchangers', Mc Grawhill Book Company, 1964